JACS
JOURNAL OF THE AMERICAN CHEMICAL SOCIETY
Communication
pubs.acs.org/JACS

# Enhanced Photoelectrochemical Water Oxidation on Bismuth Vanadate by Electrodeposition of Amorphous Titanium Dioxide

David Eisenberg, Hyun S. Ahn, and Allen J. Bard*

Center for Electrochemistry, Department of Chemistry, The University of Texas at Austin, Austin, Texas 78712, United States

Supporting Information

**ABSTRACT:** *n*-$BiVO_4$ is a promising semiconductor material for photoelectrochemical water oxidation. Although most thin-film syntheses yield discontinuous $BiVO_4$ layers, back reduction of photo-oxidized products on the conductive substrate has never been considered as a possible energy loss mechanism in the material. We report that a 15 s electrodeposition of amorphous $TiO_2$ (*a*-$TiO_2$) on W:$BiVO_4$/F:$SnO_2$ blocks this undesired back reduction and dramatically improves the photoelectrochemical performance of the electrode. Water oxidation photocurrent increases by up to 5.5 times, and its onset potential shifts negatively by ∼500 mV. In addition to blocking solution-mediated recombination at the substrate, the *a*-$TiO_2$ film—which is found to lack any photocatalytic activity in itself—is hypothesized to react with surface defects and deactivate them toward surface recombination. The proposed treatment is simple and effective, and it may easily be extended to a wide variety of thin-film photoelectrodes.

Artificial photosynthesis—the capture, conversion, and storage of solar energy in chemical bonds—is a central research theme in the field of renewable energy utilization.[1,2] Photoelectrochemistry (PEC) on semiconductor electrodes is a promising strategy for using photon energy to drive endoergic reactions, thus storing it in a "solar fuel".[3] Water splitting ($H_2O \rightarrow H_2 + {}^1/_2\,O_2$) is a heavily researched transformation for this purpose, and its photocatalysis by devices made from earth-abundant materials is of utmost fundamental and technological importance. Among candidate semiconductor materials for photosynthetic electrodes, *n*-type $BiVO_4$ has recently attracted broad attention as a robust and inexpensive photocatalyst for water oxidation.[4,5] Its advantages include absorption in the visible light range (bandgap ∼2.4 eV) and valence band edge sufficiently positive relative to the water oxidation potential.[6] The relatively slow electron transport in $BiVO_4$ can be improved by donor-type doping, e.g., with tungsten or molybdenum,[7,8] but slow charge transfer to solution remains the performance bottleneck, especially in driving complex reactions such as water oxidation.[5,6] In the absence of co-catalysts, transfer of photogenerated holes to the solution (Scheme 1, process a) might be too slow to compete with electron−hole recombination, thus decreasing the efficiency of the light-to-current conversion.[9] Recombination may occur either in the bulk of $BiVO_4$ (Scheme 1b),[10] or at defects, many of which are present at the surface in the high-surface-area films

**Scheme 1. Photo-oxidation (R + $h^+ \rightarrow$ O) and Possible Electron−Hole Recombination Pathways on W:$BiVO_4$/FTO Photoanode**

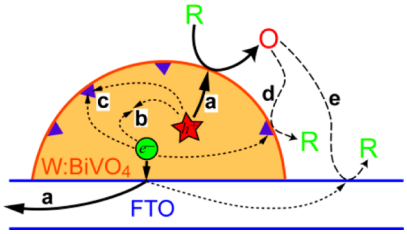


(surface recombination, Scheme 1c).[11] Further efficiency loss can occur by solution-mediated recombination when photo-oxidation products in solution are reduced back, either at surface defects (Scheme 1d), or, if the thin film is porous, at exposed regions of the underlying conductive substrate (Scheme 1e).

Most methods for $BiVO_4$ synthesis, whether chemical or physical, yield discontinuous films, where the underlying conductive substrate (typically F-doped $SnO_2$, FTO) is clearly exposed to the solution between the photocatalyst particles (Figure 1).[8,14,15] Surprisingly, solution-mediated recombination through back reduction on exposed FTO has not been considered explicitly as an energy loss mechanism for photosynthetic semiconductor electrodes, neither for $BiVO_4$ nor for other important—and often discontinuous—visible absorbing oxides such as *n*-$Fe_2O_3$, *n*-$WO_3$, and *p*-$Cu_2O$. While back reduction on the conductive substrate does affect, to varying degrees, the performance of $TiO_2$-based dye-sensitized solar cells (DSSCs),[12,13] the effect is expected to be more pronounced for photosynthetic electrodes. In the latter, the exposed substrate surface area is much larger (relative to semiconductor surface area) than in DSSCs, and the distance photo-oxidized molecules need to diffuse to FTO to be reduced is much smaller (up to 300 nm in single-layer W:$BiVO_4$, such as in Figure 1a; a small molecule crosses this distance in up to ∼50 μs).[18]

Back reduction of photo-oxidized intermediates at exposed regions of conductive substrate could be blocked by depositing a partially insulating film, as either an underlayer (before semiconductor film deposition)[12,13,19] or an overlayer (covering both semiconductor and substrate),[20,21] or by selective deposition between semiconductor particles. Nonselective

**Received:** August 11, 2014
**Published:** September 22, 2014

   dx.doi.org/10.1021/ja5082475 | J. Am. Chem. Soc. 2014, 136, 14011−14014

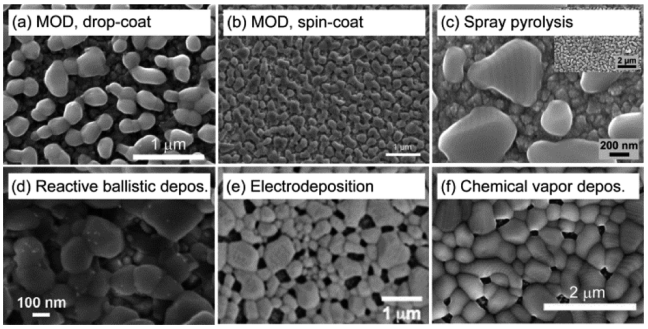


**Figure 1.** Scanning electron micrographs of some discontinuous $BiVO_4$ films, (a) prepared in our laboratory by metal−organic decomposition (MOD) in drop-cast precursor solution (doped 5% W), and (b−f) reported in the literature: (b) Gamelin et al., MOD with multiple spin coating cycles;[14] (c) van de Krol et al., spray pyrolysis of metal−organic precursors;[15] (d) Mullins et al., reactive ballistic deposition from metal precursors (doped 2% W, 6% Mo);[8] (e) Choi et al., electrodeposition;[16] (f) Ager et al., chemical vapor deposition from Bi and $V_2O_5$.[17] Figures reproduced from the cited works with permission from the ACS[14,15] and PCCP Owner Societies.[8,16,17]

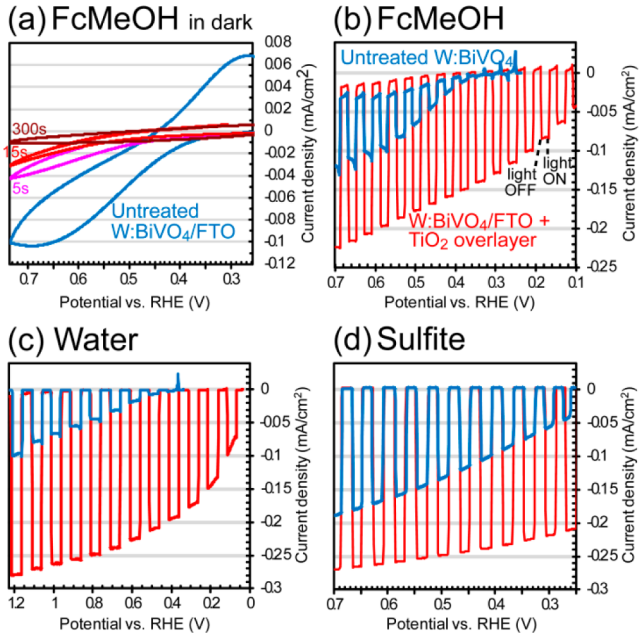


**Figure 2.** Photoelectrochemistry of W:$BiVO_4$/FTO in 0.1 M, pH 7.0 phosphate buffer, before (blue trace) and after (red trace, unless stated otherwise) electrodeposition of *a*-$TiO_2$. (a) Cyclic voltammetry in the dark of 1 mM FcMeOH, before and after 5, 15, and 300 s depositions (magenta, red, and brown traces, respectively), scan rate 50 mV/s. (b) Linear scan voltammetry (LSV) of same solution under chopped illumination. (c) Chopped light LSV of water oxidation. (d) Chopped light LSV of 0.1 M $Na_2SO_3$. Illumination by unfiltered white light from xenon lamp, 40 mW/cm$^2$. Scan rate 25 mV/s and deposition time 15 s, unless stated otherwise.

deposition introduces new, uncontrolled interfaces: between substrate and semiconductor (for an underlayer)[22] or between semiconductor and solution (for an overlayer).[20,23] A selective deposition, insulating exposed substrate regions exclusively, has been demonstrated for microwire array solar cells through two-step coverage and etching;[24,25] this approach is feasible only for high-aspect-ratio semiconductors. An alternative method for insulating the underlying substrate exclusively is electrodeposition, which utilizes the inability of *n*-type semiconductors (such as $BiVO_4$) to promote oxidations in the dark; thus, monomers are oxidized only at exposed FTO regions, insulating them selectively. This method has been employed with organic polymers to improve DSSCs performance.[16] However, poly(*o*-phenylenediamine)[26,27] films we have deposited on W:$BiVO_4$/FTO for this purpose have been unstable under PEC conditions. Thus, we have turned our attention to a robust inorganic film: amorphous $TiO_2$ (*a*-$TiO_2$).

Thin-film W-doped $BiVO_4$ photo-anodes were prepared by drop-casting a solution of $Bi^{3+}$ and $V^{3+}$ salts on a FTO-coated glass slide and annealing at 500 °C/3 h. A scanning electron micrograph (Figures 1a and S6) reveals that the annealed film is discontinuous, with W:$BiVO_4$ particles surrounded by exposed FTO substrate. To test the contribution of the exposed FTO to reactivity in solution, we measured the cyclic voltammetry (CV) of ferrocenemethanol (FcMeOH) in the dark (Figure 2a). In the absence of external excitation, the low concentration of holes in *n*-type W:$BiVO_4$ prevents it from promoting a dark oxidation. Thus, the observed oxidation wave is assigned to FTO regions which are exposed to the solution through discontinuities in the W:$BiVO_4$ layer.

Amorphous $TiO_2$ was deposited on the W:$BiVO_4$/FTO electrode by applying 0.02 V vs SCE in an acidic (pH 2.45 ± 0.03) solution of 15 mM $TiCl_3$, in the dark, for a duration of 15−30 s (Figure S1).[28,29] Since *n*-W:$BiVO_4$ is not oxidizing in the dark, $Ti^{3+}$ species are oxidized at exposed FTO regions, and the growth of the ion conducting film probably initiates there.[30] A short drying in air (30−40 min) converts the hydrated $TiO_x$ film to insulating *a*-$TiO_2$.[29] In the absence of a high-temperature annealing step, the film remains amorphous, as confirmed by X-ray diffraction (Figure S2). X-ray photoelectron spectroscopy (XPS) revealed a binding energy of 458.9 eV for the Ti $2p_{3/2}$ state (Figure S3), assigned to Ti(IV) in $TiO_2$.[29]

Electrodeposition times as short as 15 s are sufficient for blocking over 70% of the oxidation current and nearly 100% of the back reduction (Figure 2a). The rapid redox kinetics and fast diffusion rate of the FcMeOH/$FcMeOH^+$ couple render it especially sensitive to back reduction, and thus the perfect limiting case for gauging efficiency of FTO insulation. Following electrodeposition of *a*-$TiO_2$, photo-oxidation of FcMeOH on the photo-anode was improved significantly (Figure 2b): the onset potential shifted negative by at least 300 mV, and the short-circuit photocurrent increased by a factor of 10 (measured at $E^\circ$(FcMeOH/$FcMeOH^+$) = 0.42 V vs RHE).

The *a*-$TiO_2$ electrodeposition also effects a dramatic improvement in the photo-oxidation of water (Figure 2c) and of hole-scavenging sulfite ($SO_3^{2-}$, Figure 2d). Films deposited for 15−30 s shift the onset of water oxidation negatively by about 500 mV, from 0.4 to ca. −0.1 V vs RHE, while the short-circuit photocurrent increases by up to a factor of 5.5, as measured at $E^\circ$($H_2O/O_2$) = 0.82 V vs RHE at pH 7.0. The fill factor for water photo-oxidation improves from 23% to 44% following *a*-$TiO_2$ deposition. The enhanced water oxidation photocurrent was stable for very long times (>12 h, Figure S4).

Reactivity of FTO films is known to vary between samples,[13] as we have also observed by CV of FcMeOH at different W:$BiVO_4$/FTO electrodes (Figure S5). Thus, the best photoelectrochemical improvements (short-circuit photocurrent increase factors of 2.5−5.5) were obtained from a range of deposition times (15−30 s) and a range of deposition charge passed (1.8−3.6 mC/cm$^2$).


dx.doi.org/10.1021/ja5082475 | J. Am. Chem. Soc. 2014, 136, 14011−14014

Blocking of solution-mediated recombination on FTO by insulating exposed regions contributes to the boost in PEC performance, especially at low enough bias (for the FTO to reduce the photo-oxidized products) and for kinetically reversible redox couples (such as FcMeOH and possibly intermediates in the water oxidation reaction). However, this effect cannot fully account for the improvement, since back reduction loses significance at bias more positive than the reduction potential of the active redox species. Moreover, the highly irreversible oxidation of sulfite, which is less likely to be affected by blocking the back reduction, does enhance significantly following the *a*-$TiO_2$ deposition (Figure 2d). Thus, some additional beneficial effect of the *a*-$TiO_2$ over layer is present.

To shed light on this effect, we monitored the growth of *a*-$TiO_2$ by scanning electron microscopy (SEM) at different deposition times. The SEM images (Figure 3) reveal that even

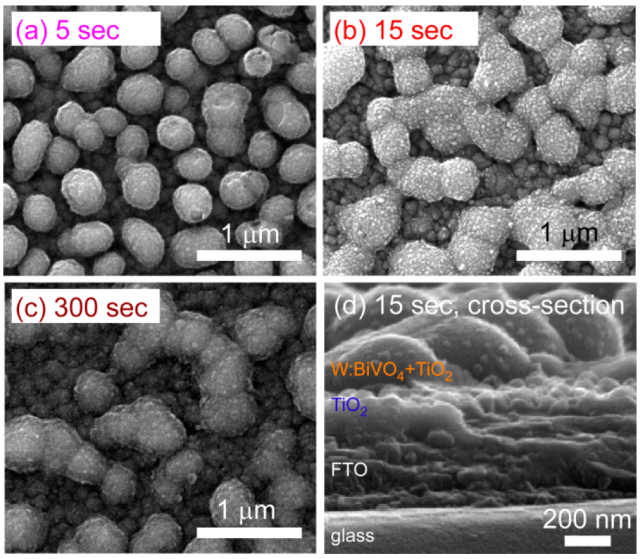


**Figure 3.** (a–c) Scanning electron micrographs of W:$BiVO_4$ at different stages of *a*-$TiO_2$ electrodeposition (deposition times given in the figure). (d) Cross-section of *a*-$TiO_2$/W:$BiVO_4$/FTO after a 15 s deposition.

after a brief, 5-s-long deposition, a layer of *a*-$TiO_2$ covers both FTO and the W:$BiVO_4$ grains. The mechanism by which *a*-$TiO_2$ covers W:$BiVO_4$ is unknown: the film might initiate at FTO regions and creep on the thin W:$BiVO_4$ grains, as suggested by SEM of lower coverage regions (Figure S7); conversely, oxidation of $Ti^{3+}$ might occur at W:$BiVO_4$ surface defects, where local Fermi level pinning may allow for a high surface hole concentration even in the dark. In the optimal deposition time range, the *a*-$TiO_2$ film is rough (Figure 3b,d), while shorter depositions (5 s, <1.8 mC/$cm^2$) afford smoother films and do not cover the grains entirely (Figure 3a). Film thickness is estimated to be 80–120 nm on the basis of cross-section SEM (Figure 3d).

Although the short (5 s) depositions are sufficient for blocking FTO reactivity (Figure 2b), they do not improve photocurrent for water oxidation significantly (Figure S8), further confirming that FTO insulation alone cannot account for the entire photocurrent enhancement. Long deposition times (>50 s, >3.6 mC/$cm^2$) cover the entire sample by a thick, rough *a*-$TiO_2$ layer (Figure 3c) and fail to improve water oxidation photocurrents (Figure S9). This is attributed to increased resistance of the *a*-$TiO_2$, blocking charge transfer to the solution. Thus, 15–30 s deposition times strike an optimal balance between resistance and surface coverage.

To test whether the electrodeposited *a*-$TiO_2$ acts as a photocatalyst, it was electrodeposited directly on FTO. The *a*-$TiO_2$ layer, whose presence was confirmed by decreased FcMeOH oxidation current, showed no photoresponse whatsoever (Figure S11). Moreover, the *a*-$TiO_2$ layer did not contribute significantly to light absorption on W:$BiVO_4$/FTO, as measured by UV–vis spectroscopy (Figure S12) and by plotting incident photon-to-current efficiency (IPCE, Figure S13). Overall, these observations suggest that *a*-$TiO_2$ is neither a photocatalyst nor a photosensitizer to the W:$BiVO_4$.

Addition of $Co_3O_4$ nanoparticles (11 nm, synthesized in autoclave[31] and drop-cast on *a*-$TiO_2$-covered W:$BiVO_4$) further improved the water oxidation photocurrent (Figure S15). However, the *a*-$TiO_2$ film alone—although not catalytic in itself—contributes an appreciable part of the total observed photoelectrochemical improvement (75% at 0.82 V vs RHE, Figure 2c), underscoring the effectiveness of the treatment.

The PEC enhancement may best be explained by a combination of two mechanisms: (1) FTO insulation, which blocks solution-mediated recombination at the FTO (Scheme 1e), and (2) chemical treatment of W:$BiVO_4$ surface defects, which may block them from participating in electron–hole surface recombination (Scheme 1c) and in solution-mediated recombination (Scheme 1d). Surface defects have been observed in $BiVO_4$,[8,32] and might be of either chemical or structural nature, ranging from dopant segregates to grain boundaries. Chemical passivation for treating such defects has been shown to improve PEC performance in various photoelectrodes.[33–35] In the case of $BiVO_4$, most surface treatments in the literature consist of catalyst deposition;[5,6] however, two noncatalytic surface treatments (by Ag metal[36,37] and $NiO_x$[38]) have been shown previously to improve its performance by blocking surface recombination (although to a lesser extent than the *a*-$TiO_2$ treatment reported here).

Another possible contribution to PEC enhancement may arise from improved charge collection due to band-bending at the *a*-$TiO_2$–$BiVO_4$ interface, as has been observed in crystalline $TiO_2$–$BiVO_4$ composites.[39] Furthermore, the *a*-$TiO_2$ layer may introduce band-bending defects (such as oxygen vacancies), which might further contribute to electron–hole separation.[40]

To explain the conductivity of *a*-$TiO_2$, we recall that chemically deposited, unannealed $TiO_2$ is a known "leaky dielectric".[41,42] *a*-$TiO_2$ layers contain numerous electronic defects, arising from oxygen vacancies, presence of $Ti^{3+}$ ions in the lattice, and contaminations (specifically, chlorine from titanium chloride-based preparations).[41–43] This property probably explains the conductivity of our *a*-$TiO_2$ film, as it is clearly too thick to allow tunneling. Recently, an amorphous $TiO_2$ film (prepared by atomic layer deposition and not annealed) was shown to be a very good conductor of holes on several semiconductor photoelectrodes.[43]

In summary, we report that electrodeposition of amorphous $TiO_2$ boosts the photoelectrochemical performance of a W:$BiVO_4$/FTO photo-anode toward the oxidation of water, kinetically reversible FcMeOH, and hole-scavenging sulfite. *a*-$TiO_2$ over layers of optimal thickness (80–120 nm, deposited for 15–30 s, with 1.8–3.6 mC/$cm^2$ charge passed) increased the water oxidation photocurrent by a factor of up to 5.5, shifted the onset potential negatively by ~500 mV, increased the fill factor to 44%, and were stable for at least 12 h. The *a*-


dx.doi.org/10.1021/ja5082475 | J. Am. Chem. Soc. 2014, 136, 14011–14014

$TiO_2$ layer grows in the dark, possibly from exposed FTO regions, and its optimal thickness balances between sufficient surface coverage and minimal resistance to charge transfer to solution. This beneficial effect of the *a*-$TiO_2$ overlayer, which is not photo-active, is attributed to blocking of surface recombination and to solution-mediated recombination at surface defects and at exposed regions of the conductive substrate. Current research is directed toward characterization of this phenomenon. Since many semiconductor thin-film electrodes are discontinuous, this treatment may benefit a wide range of photocatalytic systems and devices.

## ■ ASSOCIATED CONTENT

### Supporting Information

Experimental procedures, and Figures S1−S15. This material is available free of charge via the Internet at http://pubs.acs.org.

## ■ AUTHOR INFORMATION


### Corresponding Author

ajbard@mail.utexas.edu


### Notes

The authors declare no competing financial interest.

## ■ ACKNOWLEDGMENTS

We thank Drs. N. Klein, J. Kim, C. Renault, and N. Eisenberg for valuable discussions, glass experts M. Ronalter and A. V. Kennedy for varied technical help, Dr. H. Celio for the XPS measurement, Dr. V. M. Lynch for the XRD measurement, and A. J. E. Rettie, C. J. Stolle, and Dr. B. A. Korgel for the UV−vis spectroscopy measurements. This work was financially supported by California Institute of Technology (no. 68D-1094596).

## ■ REFERENCES


(1) Bard, A. J.; Fox, M. A. *Acc. Chem. Res.* **1995**, *28*, 141.
(2) Nocera, D. G. *Acc. Chem. Res.* **2012**, *45*, 767.
(3) Walter, M. G.; Warren, E. L.; McKone, J. R.; Boettcher, S. W.; Mi, Q.; Santori, E. A.; Lewis, N. S. *Chem. Rev.* **2010**, *110*, 6446.
(4) Kudo, A.; Omori, K.; Kato, H. *J. Am. Chem. Soc.* **1999**, *121*, 11459.
(5) Park, Y.; McDonald, K. J.; Choi, K.-S. *Chem. Soc. Rev.* **2013**, *42*, 2321.
(6) Li, Z.; Luo, W.; Zhang, M.; Feng, J.; Zou, Z. *Energy Environ. Sci.* **2013**, *6*, 347.
(7) Park, H. S.; Kweon, K. E.; Ye, H.; Paek, E.; Hwang, G. S.; Bard, A. J. *J. Phys. Chem. C* **2011**, *115*, 17870.
(8) Berglund, S. P.; Rettie, A. J. E.; Hoang, S.; Mullins, C. B. *Phys. Chem. Chem. Phys.* **2012**, *14*, 7065.
(9) Ma, Y.; Pendlebury, S. R.; Reynal, A.; Le Formal, F.; Durrant, J. R. *Chem. Sci.* **2014**, *5*, 2964.
(10) Vinke, I. C.; Diepgrond, J.; Boukamp, B. A.; De Vries, K. J.; Burggraaf, A. J. *Solid State Ionics* **1992**, *57*, 83.
(11) Liu, R.; Zheng, Z.; Spurgeon, J.; Yang, X. *Energy Environ. Sci.* **2014**, *7*, 2504.
(12) Gregg, B. A.; Pichot, F.; Ferrere, S.; Fields, C. L. *J. Phys. Chem. B* **2001**, *105*, 1422.
(13) Cameron, P. J.; Peter, L. M.; Hore, S. *J. Phys. Chem. B* **2005**, *109*, 930.
(14) Zhong, D. K.; Choi, S.; Gamelin, D. R. *J. Am. Chem. Soc.* **2011**, *133*, 18370.
(15) Liang, Y.; Tsubota, T.; Mooij, L. P. A.; van de Krol, R. *J. Phys. Chem. C* **2011**, *115*, 17594.
(16) Choi, S. K.; Choi, W.; Park, H. *Phys. Chem. Chem. Phys.* **2013**, *15*, 6499.
(17) Alarcón-Lladó, E.; Chen, L.; Hettick, M.; Mashouf, N.; Lin, Y.; Javey, A.; Ager, J. W. *Phys. Chem. Chem. Phys.* **2014**, *16*, 1651.
(18) Bard, A. J.; Faulkner, L. R. *Electrochemical Methods: Fundamentals and Applications*; John Wiley & Sons: New York, 2011.
(19) Kavan, L.; Grätzel, M. *Electrochim. Acta* **1995**, *40*, 643.
(20) Kay, A.; Grätzel, M. *Chem. Mater.* **2002**, *14*, 2930.
(21) Liberatore, M.; Burtone, L.; Brown, T. M.; Reale, A.; Di Carlo, A.; Decker, F.; Caramori, S.; Bignozzi, C. A. *Appl. Phys. Lett.* **2009**, *94*, No. 173113.
(22) Ito, S.; Ishikawa, K.; Wen, C.-J.; Yoshida, S.; Watanabe, T. *Bull. Chem. Soc. Jpn.* **2000**, *73*, 2609.
(23) Yum, J.-H.; Moehl, T.; Yoon, J.; Chandiran, A. K.; Kessler, F.; Gratia, P.; Grätzel, M. *J. Phys. Chem. C* **2014**, *118*, 16799.
(24) Kelzenberg, M. D.; Turner-Evans, D. B.; Putnam, M. C.; Boettcher, S. W.; Briggs, R. M.; Baek, J. Y.; Lewis, N. S.; Atwater, H. A. *Energy Environ. Sci.* **2011**, *4*, 866.
(25) Shin, J. C.; Kim, K. H.; Yu, K. J.; Hu, H.; Yin, L.; Ning, C.-Z.; Rogers, J. A.; Zuo, J.-M.; Li, X. *Nano Lett.* **2011**, *11*, 4831.
(26) Yacynych, A. M.; Mark, H. B., Jr. *J. Electrochem. Soc.* **1976**, *123*, 1346.
(27) Long, J. W.; Rhodes, C. P.; Young, A. L.; Rolison, D. R. *Nano Lett.* **2003**, *3*, 1155.
(28) Kavan, L.; O'Regan, B.; Kay, A.; Grätzel, M. *J. Electroanal. Chem.* **1993**, *346*, 291.
(29) Kim, J.; Kim, B.-K.; Cho, S. K.; Bard, A. J. *J. Am. Chem. Soc.* **2014**, *136*, 8173.
(30) Kavan, L.; Stoto, T.; Grätzel, M.; Fitzmaurice, D.; Shklover, V. *J. Phys. Chem.* **1993**, *97*, 9493.
(31) Dong, Y.; He, K.; Yin, L.; Zhang, A. *Nanotechnology* **2007**, *18*, 435602.
(32) Flaherty, D. W.; Hahn, N. T.; May, R. A.; Berglund, S. P.; Lin, Y.-M.; Stevenson, K. J.; Dohnalek, Z.; Kay, B. D.; Mullins, C. B. *Acc. Chem. Res.* **2012**, *45*, 434.
(33) Parkinson, B. A.; Heller, A.; Miller, B. *Appl. Phys. Lett.* **1978**, *33*, 521.
(34) Seager, C. H.; Ginley, D. S. *Appl. Phys. Lett.* **1979**, *34*, 337.
(35) Kay, A.; Cesar, I.; Grätzel, M. *J. Am. Chem. Soc.* **2006**, *128*, 15714.
(36) Sayama, K.; Nomura, A.; Arai, T.; Sugita, T.; Abe, R.; Yanagida, M.; Oi, T.; Iwasaki, Y.; Abe, Y.; Sugihara, H. *J. Phys. Chem. B* **2006**, *110*, 11352.
(37) Park, H. S.; Lee, H. C.; Leonard, K. C.; Liu, G.; Bard, A. J. *ChemPhysChem* **2013**, 2277.
(38) Liang, Y.; Messinger, J. *Phys. Chem. Chem. Phys.* **2014**, *16*, 12014.
(39) Ho-Kimura, S.; Moniz, S. J. A.; Handoko, A. D.; Tang, J. *J. Mater. Chem. A* **2014**, *2*, 3948.
(40) Lewerenz, H. J.; Heller, A.; DiSalvo, F. J. *J. Am. Chem. Soc.* **1980**, *102*, 1877.
(41) Wilk, G. D.; Wallace, R. M.; Anthony, J. M. *J. Appl. Phys.* **2001**, *89*, 5243.
(42) Dueñas, S.; Castán, H.; García, H.; Andrés, E. S.; Toledano-Luque, M.; Mártil, I.; González-Díaz, G.; Kukli, K.; Uustare, T.; Aarik, J. *Semicond. Sci. Technol.* **2005**, *20*, 1044.
(43) Hu, S.; Shaner, M. R.; Beardslee, J. A.; Lichterman, M.; Brunschwig, B. S.; Lewis, N. S. *Science* **2014**, *344*, 1005.